Synthetic Proton-Gated Ion Channels via Single Solid-State Nanochannels Modified with Responsive Polymer Brushes

ARTICLE *in* NANO LETTERS · JULY 2009

Impact Factor: 13.59 · DOI: 10.1021/nl901403u · Source: PubMed

6 AUTHORS, INCLUDING:

Basit Yameen
Harvard Medical School
56 PUBLICATIONS **1,255** CITATIONS
SEE PROFILE

Omar Azzaroni
INIFTA-CONICET-UNLP
142 PUBLICATIONS **3,164** CITATIONS
SEE PROFILE

NANO LETTERS

2009
Vol. 9, No. 7
2788-2793

Synthetic Proton-Gated Ion Channels via Single Solid-State Nanochannels Modified with Responsive Polymer Brushes

Basit Yameen,[†] Mubarak Ali,[‡] Reinhard Neumann,[§] Wolfgang Ensinger,[‡] Wolfgang Knoll,[||] and Omar Azzaroni*,[⊥]

Max-Planck-Institut für Polymerforschung, Ackermannweg 10, 55128 Mainz, Germany, Technische Universität Darmstadt, Fachbereich Material- u. Geowissenschaften, Fachgebiet Chemische Analytik, Petersenstrasse 23, D-64287 Darmstadt, Germany, GSI Helmholtzzentrum für Schwerionenforschung GmbH, Planckstrasse 1, D-64291 Darmstadt, Germany, Austrian Institute of Technology, Donau-City-Strasse 1, 1220 (Vienna), Austria, and Instituto de Investigaciones Fisicoquímicas Teóricas y Aplicadas (INIFTA), CONICET Universidad Nacional de La Plata, CC 16 Suc.4 (1900) La Plata, Argentina

Received May 2, 2009; Revised Manuscript Received June 5, 2009

ABSTRACT

The creation of switchable and tunable nanodevices displaying transport properties similar to those observed in biological pores poses a major challenge in molecular nanotechnology. Here, we describe the construction of a fully "abiotic" nanodevice whose transport properties can be accurately controlled by manipulating the proton concentration in the surrounding environment. The ionic current switching characteristics displayed by the nanochannels resemble the typical behavior observed in many biological channels that fulfill key pH-dependent transport functions in living organisms, that is, the nanochannel can be switched from an "off" state to an "on" state in response to a pH drop. The construction of such a chemical nanoarchitecture required the integration of stable and ductile macromolecular building blocks constituted of pH-responsive poly(4-vinyl pyridine) brushes into solid state nanopores that could act as gate-keepers managing and constraining the flow of ionic species through the confined environment. In this context, we envision that the integration of environmental stimuli-responsive brushes into solid-state nanochannels would provide a plethora of new chemical alternatives for molecularly design robust signal-responsive "abiotic" devices mimicking the function of proton-gated ion channels commonly encountered in biological membranes.

During the last few years, the scientific community witnessed great interest in the study and application of nanoscale fluidic architectures in order to control and manipulate the transport of chemical and biochemical species in close resemblance to biological channels.[1−8] This endeavor together with the remarkable advances in nanofabrication techniques gave rise to different routes to construct in a reproducible manner fully "abiotic" inorganic and polymeric nanochannels with dimensions comparable to biological molecules.[9,10] Furthermore, synthetic solid-state nanochannels display several important advantages over their biological counterparts such as robustness, stability, control over channel geometry, amenable integration into devices, and tailorable surface properties.[1,4] Regarding this latter, it is worthwhile mentioning that appealing effects arise when the channel surface is charged and the dimensions are comparable to the range of the electrostatic interactions in solution.[11−13] In the case of having a channel size with dimensions smaller than the Debye length, the nanoconfined environment becomes a "unipolar solution" of counterions in order to neutralize the immobilized surface charge.[14] This implies that by controlling the surface charge density along the confined environment the channel conductance and, as a consequence, the ion current can be modulated. A key goal of nanotechnology relies on the design and construction of functional systems having properties that are specific to their size.[15] These fascinating physicochemical properties displayed by charged nanochannels provided the scenario to create new functional and addressable architectures and also led to the birth of a whole new area of research concerning the design of

* To whom correspondence should be addressed. E-mail: azzaroni@inifta.unlp.edu.ar; Web: http://softmatter.quimica.unlp.edu.ar.
[†] Max-Planck-Institut für Polymerforschung.
[‡] Technische Universität Darmstadt.
[§] GSI Helmholtzzentrum für Schwerionenforschung GmbH.
[||] Austrian Institute of Technology.
[⊥] CONICET Universidad Nacional de La Plata.

10.1021/nl901403u CCC: $40.75
Published on Web 06/11/2009

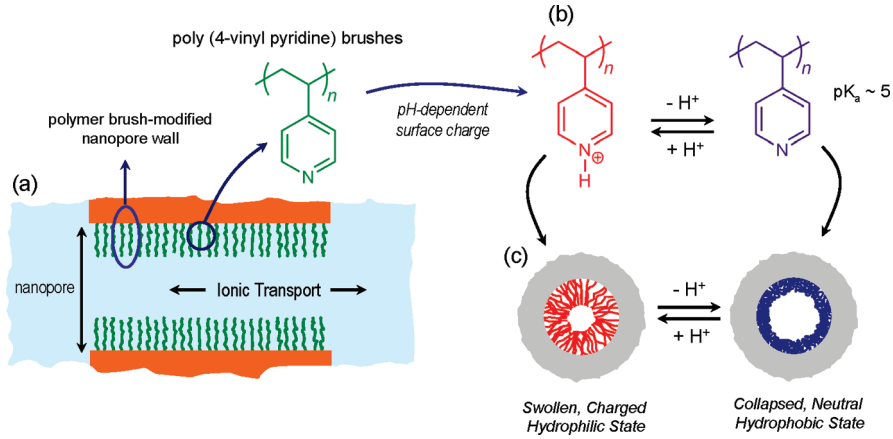

Figure 1. (a) Simplified description of the brush-modified cylindrical nanochannel. Also indicated in the scheme is the chemical structure of poly(4-vinyl pyridine) brushes. (b) pH-dependent pyridine-pyridinium equilibrium taking place in the brush environment. (c) Simplified illustration indicating the conformational changes occurring in the brush layer upon variations in the environmental pH.

nanochannel-based devices resting on surface charge-governed ionic transport, for example, nanofluidic diodes[16] or bipolar diodes.[17] Regulation of nanochannel/nanopore surface charge is a most important principle that nature also exploits to create molecular gates enabling the controlled passage of ions through the membranes. However, in the case of biological channels, the mechanisms for activating the transport of ions can be more complicated and triggered by environmental conditions.[18−20] In the presence of specific chemical stimuli, the channel/pore can be switched from an "off" state, in which no or low ionic current passes through the channels, to an "on" state that is evidenced by a high transmembrane ionic current. This gives rise to a molecular gate that is activated by an external chemical stimulus, like pH. For example, the tetrameric M2 protein from influenza A, one of the simplest pH-gated ion channels known, suffers a conformational switch upon protonation of its histidine residues.[21] The structural switch, from a uniprotonated to a biprotonated channel, causes an electrostatic repulsion between the charged histidine moieties that pushes the helices apart. More important, the pH required to activate the channel is close to the pK_a of the histidine groups, indicating that the protonation change is responsible for the channel gating.[22] This example illustrates how relevant nanochannel responsiveness is in terms of adaptability to environmental changes and tunability of electrostatic characteristics. Recently, we have demonstrated that polymer brushes represent a valuable alternative to modify the electrostatic environment of nanochannels and to significantly increase the surface density of functional groups.[23] These macromolecular films enable the facile molecular design of interfaces in order to control surface charge, hydrophobicity, and chemical functionality in an accurate manner.[24−26] In few words, they provide unique new avenues to incorporate "smart" or "responsive" chemical functionalities into confined geometries.

Within this framework, the integration of environmental stimuli-responsive brushes into solid-state nanochannels would lead to the creation of robust signal-responsive devices mimicking the function of proton-gated ion channels commonly encountered in biological membranes, that is, the nanochannel can be switched from an "off" state to an "on" state in response to a pH drop.

Here, we report the construction of a nanochannel-based chemical device whose transmembrane ion current can be accurately controlled by manipulating the proton concentration in the surrounding environment. In this context, pH-responsive poly(4-vinyl pyridine) brushes were incorporated into single solid-state nanochannels in a fashion that leads to a nanodevice whose electronic readout can be switched between "on" and "off" states. In close resemblance to biological channels, the pH required to activate the "abiotic" ion channel is close to the pK_a of the pyridine groups. The electrostatic changes arising from the protonation/deprotonation of these groups are responsible for tuning the channel conductance that leads to the gating behavior. More important, we also demonstrate that the pH can tune and amplify the electronic readout in the "on" configuration. The use of "responsive" macromolecular architectures to manipulate the ion transport through nanochannels provides an attractive strategy for creating electronic nanodevices with environmental responsive characteristics to be implemented as robust "smart" nanochannel sensors.

Single cylindrical nanochannels with diameter (d) of ~ 15 nm and length (L) of ~12 μm were fabricated by symmetrical etching of ion-tracked polyethylene terephthalate (PET) films, irradiated with single swift heavy ions.[27] Then, the single nanochannel-containing membranes were modified with 4,4′-azobis(4-cyanopentanoic acid) as a surface-confined polymerization initiator.[28,29] Afterward, the polyvinylpyridine (PVP) brush growth was accomplished by surface-initiated free radical polymerization of the pH-responsive monomer 4-vinyl pyridine (Figure 1). After a preset polymerization time, the membranes were thoroughly rinsed with deionized water and mounted between the two halves of the conductivity cell. Figure 2 depicts the $I-V$ curves of a single nanochannel modified with PVP brushes using 0.1 M KCl (at different pHs) as an electrolyte solution in both half cells. By increasing the pH from 2 to 4, and finally to 10, a significant decrease in the transmembrane ionic current was observed under the same applied bias. The pH-dependent

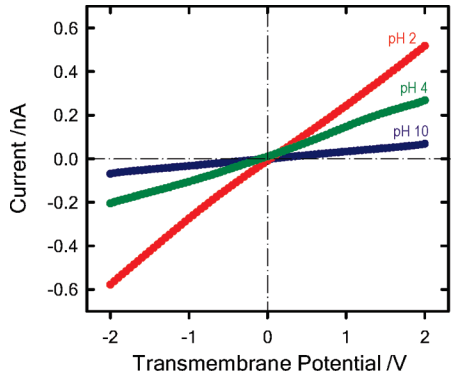

Figure 2. Current−voltage characteristics of a single cylindrical PVP brush-modified nanochannel in 0.1 M KCl at different pH's: (red circles) 2, (green circles) 4, (blue circles) 10.

$I-V$ response is correlated to channel conductance values of 0.27, 0.12, and 0.033 nS for pHs 2, 4, and 10, respectively. The conductance values of the nanochannel were determined by fitting the slope of the transmembrane current as a function of the applied voltage.[8] These results reveal that pH variations from 2 to 10 can lead to an 8-fold decrease in transmembrane ionic current from 0.52 to 0.065 nA, passing through the nanochannel.

In close resemblance to the biological example of the M2 protein, the interpretation of these results requires considering the chemical equilibrium associated to the protonation of the pyridine moieties in the brush layer. The pyridine−pyridinium equilibrium is responsible for setting the electrostatic characteristics of the molecular film covering the inner walls of the nanochannel (Figure 1). As is well known, surface charges induce electrostatic screening and electrokinetic effects that may have large effects on the channel conductance.[11] In highly confined environments with dimensions comparable to the Debye length, the surface charge density (σ) determines the local ionic concentration within the nanochannel and in this way controls the nanochannel conductance (G). The charged surface attracts the mobile counterions from the ionic solution and builds up a charged layer that screens the surface-confined charges. As a result, surface charges proportionally raise the nanochannel conductance by mediating the transport of counterions near the surface, $G \propto \sigma$. Therefore, we can infer that at strongly acidic pH values the pyridine moieties in the brush are protonated, thus conferring a well-defined cationic character to the surface charges immobilized in the inner environment of the nanochannel. As described in Figure 1, the equilibrium of the pyridine moieties, which in turn determines the population of pyridinium species, is thermodynamically controlled by the pH value. The pK_a of the pyridine−pyridinium equilibrium is 5.2.[30] So, by changing the acidic pH from 2 to 4 the population of neutral pyridine moieties grew at the expense of the pyridinium species, resulting in a "less positive" nanochannel surface. This pH-induced variation in surface charges proportionally affects the channel conductance, that is, the channel conductance decreases as the pH increases. Figure 3 shows that the displacement of the protonation equilibrium enables the modulation of the

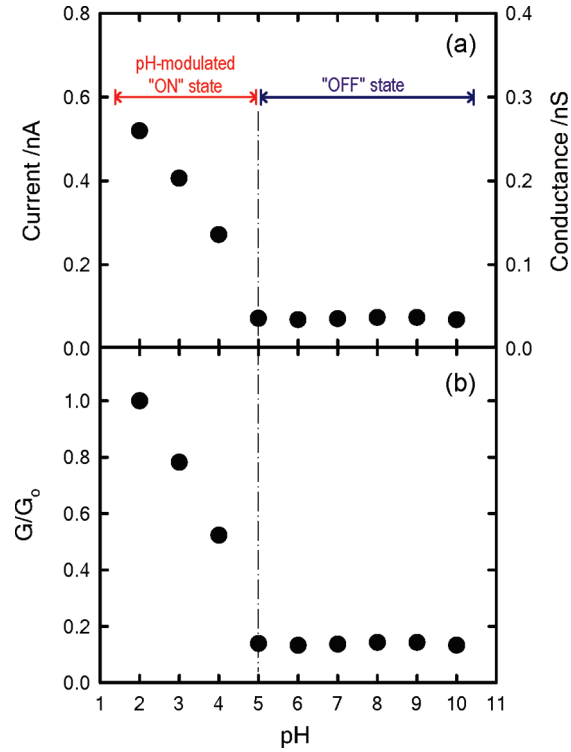

Figure 3. Representation of the transmembrane ionic current (measured at 2 V of applied bias voltage) (panel a), the nanochannel conductance (panel a), and the nanochannel conductance normalized to the maximal conductance of the "fully" open channel at pH 2 (G/G_o) (panel b) as a function of the environmental pH for a PVP brush-modified cylindrical nanochannel. In the plot are also indicated the regions corresponding to the "on" and "off" states of the nanogate. The dotted vertical line at pH 5 ($\sim pK_{aPy-Py+}$) was introduced to guide the eye. The error bars are smaller that the symbol size.

transmembrane ionic current by changes in the proton concentration in the range $2 \leq$ pH ≤ 5.

The decreasing variation in transmembrane current is 0.147 nA/pH unit. This indicates that the pH-controlled pyridine/pyridinium equilibrium provides a facile chemical tool to easily tune the electronic readout originating from the ionic transport through the nanochannel. The magnitude of the transmembrane ion currents and channel conductivities at different pHs are highly reproducible, indicating the fidelity and robustness of the PVP brush to control the ion transport through the nanochannel. After that, increasing the pH above pK_a caused no further changes in the transmembrane current values. As is evident from figure 3, the transmembrane current decreases with increasing proton concentration until reaching the condition pH $\sim$ pK_a, in which the nanochannel displays the lowest conductance value, 33 pS. Then, a constant low conductance value in the range $5 \leq$ pH ≤ 10 was observed. This can be interpreted considering that the equilibrium of the PVP brush has been fully displaced toward the formation of uncharged pyridine and, consequently, the surface charges which mediated the transport of counterions near the surface and boosted the channel conductance were removed from the channel. As such, the full deprotonation of the PVP brush led to the "off" state (low conductance) of the nanochannel. In our experimental scenario, the trans-

membrane ion currents in the "off" and "on" states differ by nearly 1 order of magnitude, thus indicating that the pH-induced physicochemical changes, undergone by the brush, enable the opening and closure of the gate. Figure 3b shows the channel conductance normalized to the maximal conductance of the "fully" open channel at pH 2, G/G_o, plotted against the environmental pH. The chemical actuation of the ionic gate from the "on" to the "off" state promotes 87% decrease in channel conductance. These relative changes in channel conductance measured in the PVP brush-modified nanochannel are comparable to that observed in many biological systems, as is the case of the proton-gated Na^+ current in patch-clamped Calu-3 cells, which display ~90% decrease in ion current upon closing their channels.[31] Regarding this latter, it is worthwhile mentioning that the geometric characteristics and dimensions of the synthetic pores differ from those observed in biological channels. The length of the synthetic nanopores is nearly 3 orders of magnitude larger than that encountered in biological ion channels. As such, even though the design concept presented here would be viable for shorter pores, a direct comparison of the opening/closure characteristics of both systems is not completely fair.

It should be also borne in mind that deprotonation of PVP not only promotes the removal of the surface charges but also leads to a sharp transition of the swollen hydrophilic brush into a collapsed hydrophobic state.[32] In principle, the structural reorganization into a collapsed state would change the effective cross section of the channel that would lead to a slight increase in channel conductivity. As can be seen in Figure 3, collapsing the brush above pH 5 does not reflect any increase in conductivity. This indicates that the cross-sectional changes, that is, variations in the nanochannel effective diameter, which may occur as a result of the brush conformational change (collapse), are not significant when compared with the major electrostatic changes promoted by the deprotonation of the pyridinium moieties. Furthermore, the collapse of the PVP brushes promotes major changes in the hydrophobicity of the surface. Recently, Lindqvist et al. reported that the wettability of surfaces modified with PVP brushes can be switched from 0 to 120° upon variations in pH from 3 to 9.[33] This indicates that increasing the pH above pK_a switches the inner environment of the nanochannel from a hydrophilic conducting "on" state to a hydrophobic nonconducting "off" state. We hypothesize that by decreasing the polarity of the channel wall, that is, increasing its hydrophobicity, could act as an effective mechanism to hinder the formation of the mobile electrolyte layer that mediates the ionic transport in the boundaries of the channel wall.[34] In addition, we have to note that water in very confined geometries can exhibit different dynamics not seen in the bulk system, including the wet−dry transition due to confinement.[35] Recent experimental work reported by Dekker and co-workers described the anomalous conductance behavior of nanochannels ~10 nm in diameter.[36] This behavior was attributed to the presence of air nanobubbles trapped inside the nanochannels. In a similar fashion, Russo et al. suggested that the bubbles can act as bistable hydrophobic gates responsible for the on−off transitions of single channel currents.[37] In our case, we did not observe any fluctuations in the channel conductivity at any fixed pH, which might indicate that no nanobubbles are present. Reversing the pH of the solution reflects highly reproducible and reversible changes in the transmembrane ion currents flowing through the macromolecular gate operating in the "on" and "off" states (Figure 4). The difference in amplitude between the higher conductance state and the lower one is remarkably constant.

In summary, we have described here the construction of a fully "abiotic" nanodevice displaying the ionic current switching behavior typical of that observed in many biological channels that fulfill key pH-dependent transport functions in living organisms. Construction of such a nanodevice required the integration of stable and ductile macromolecular building blocks with the appropriate responsiveness that could act as gate-keepers managing and constraining the flow of ionic species through the confined environment. Our approach employed dressing of the inner walls of PET-made single nanochannels with pH-responsive poly (4-vinyl pyridine) brushes. The "on/off" switching was based on the manipulation of the surface charges of the channel walls via the protonation of the brush layer, which in turn control the channel conductivity. The externally controllable switch was chemically actuated through environmental pH changes with which the gate is opened or closed. In the range $2 \leq pH \leq 5$, the measurable electronic readout was modulated with gradual changes in the proton concentration, thus leading to a pH-tunable transmembrane ionic current. Increasing the pH above the pK_a of the pyridine moieties led to the full deprotonation of the nanochannel, which gave rise to the closure of the ionic gate.

The development of chemically actuated nanovalves with tunable properties resulting from charge and macromolecular changes provides an attractive avenue to design and construct robust nanoscale systems resembling the functions of sophisticated biological structures like channel-forming proteins. In this context, we believe that the use of responsive polymer bushes, incorporated into solid-state single nanochannels, represents an exciting approach to create tailor-made nanovalves to be implemented in sensoring, dosing, signal transduction or nanofluidic systems.

Experimental Section. ***Materials and Methods.*** 4,4′-Azobis(4-cyanopentanoic acid), purum ≥98.0%, (Fluka), *N*,*N*'-dicyclohexylcarbodiimide (DCC), puriss., ≥99.0% (GC) (Fluka), *N*-(3-dimethylaminopropyl)-*N*′-ethylcarbodiimide hydrochloride 98%, (Fluka), pentafluorophenol (PFP) +99%, and 4-vinylpyridine 95% (Aldrich) were obtained from Sigma-Aldrich, Schnelldorf, Germany. Dry *N*,*N*-dimethyl formamide (DMF) was obtained from Acros Organics, Geel, Belgium. Ethylenediamine 99+ % was obtained from Merck, Germany. Polyethylene terephthalate, PET (Hostaphan RN 12, Hoechst, Germany) membranes of 12 μm thickness, were irradiated at the UNILAC linear accelerator (GSI, Darmstadt) with single swift heavy ions (Pb, U) of energy 11.4 MeV/u.

Cylindrical Nanochannel Fabrication. In order to obtain a cylindrical channel, the single heavy ion-irradiated PET membrane was symmetrically etched from both sides in a double-walled beaker filled with etchant (2 M NaOH) for 4 min. The temperature of the etching solution was adjusted at 50 °C by a circuit of heated water flowing through the double walls of the beaker. Then, the etched membranes were thoroughly washed with distilled water. Subsequently, the membranes were immersed in deionized water overnight in order to remove the residual salts. Before functionalization, the diameter of the track-etched channel was determined from its ionic conductance using 1 M KCl electrolyte solution.[27]

Functionalization with Ethylenediamine. The above-described etching procedure results in the generation of carboxyl groups on the wall of the nanochannel. During activation, these carboxyl groups were converted into pentafluorophenyl esters. For this, an ethanolic solution containing 0.1 M EDC and 0.2 M PFP was placed on both sides of the track-etched single nanochannel-membrane that was mounted between the two halves of a conductivity cell. The activation was carried out for 1 h at room temperature. After washing with ethanol several times, the solution was replaced with 0.1 M ethylendiamine (EDA) on both sides of the membrane and left overnight. Then, the modified membrane was washed three times with ethanol followed by careful rinsing with deionized water.

Anchoring of 4,4′-azobis(4-cyanopentanoic acid) on the Single Nanochannel-Containing PET Membrane. A 0.5 g sample (1.78 mmol) of 4,4′-Azobis(4-cyanopentanoic acid) and 0.92 g (4.5 mmol) of DCC were added to a single-neck Schlenk flask and closed with a rubber septum. The reactants were degassed under vacuum for 15 min followed by backfilling with N_2(g). Forty milliliters of dry DMF was added to the flask through the septum with the help of a syringe, and the reactants were allowed to dissolve. After complete dissolution, 0.13 mL of dry pyridine was added. The membrane with a single cylindrical aminated nanochannel was sealed in a Schlenk tube and degassed (4× high vacuum pump/N_2 refill cycles). The polymerization solution was syringed into this Schlenk flask, adding enough solution to fully cover the membrane, and left for 12−15 h under N_2(g) at room temperature. Then, the initiator-functionalized membrane was removed from the reaction mixture and immersed in a beaker containing DMF. The beaker was gently shaken over a period of 2 h. The membrane was then washed twice with DMF followed by washing with water and ethanol (twice each). The initiator-functionalized membrane was stored under nitrogen at 4 °C until further use.

Poly-4-vinylpyridine Brush Growth. In a 50 mL Schlenk flask, 8 g of the 4-vinylpyridine (previously passed through basic alumina) was dissolved in 10 mL of ethanol. The solution was degassed by N_2(g) bubbling for 1 h. The initiator functionalized single cylindrical-nanochannel membrane was sealed in a Schlenk tube and degassed (4× high vacuum pump/N_2 refill cycles). The monomer solution was syringed into this Schlenk flask adding enough liquid to fully cover the membrane. The flask was immersed in an oil bath preheated to 65 °C. The polymerization was carried out at 65 °C for 45 min. The PVP-modified nanochannel membrane was then removed from the polymerization solution and thoroughly rinsed with ethanol. The poly-4-vinylpyridine brush grafted membrane was stored in water until further use.

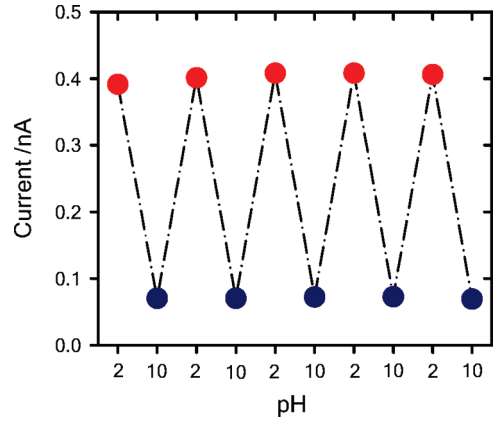

Figure 4. Reversible variation of the transmembrane ionic current passing through the PVP brush-modified nanochannel upon alternating the environmental pH between 2 (red circles, "on" state) and 10 (blue circles, "off" state). The error bars are smaller than the symbol size.

Current−Voltage Measurements. The single nanochannel membranes modified with PVP brushes were mounted between the two halves of the conductivity cell and both halves of the cell were filled with 0.1 M KCl solution. The pH of the electrolyte was adjusted by dilute HCl or KOH solutions. A Ag/AgCl electrode was placed into each half-cell solution, and a picoammeter/voltage source (Keithley 6487, Keithley Instruments, Cleveland, OH) was used to apply the desired transmembrane potential. To measure the resulting ion current flowing through the nanochannel, a scanning triangle voltage from −2 to +2 V on the tip side was applied (the base side of the channel remained connected to the ground electrode).

Acknowledgment. B.Y. acknowledges support from the Higher Education Commission (HEC) of Pakistan and Deutscher Akademischer Austauschdienst (DAAD) (Code No. A/04/30795). M.A. thanks the Higher Education Commission (HEC) of Pakistan on receiving partial financial support. O.A. is a CONICET fellow and acknowledges financial support from the Max Planck Society (Germany), the Alexander von Humboldt Stiftung (Germany), and the Centro Interdisciplinario de Nanociencia y Nanotecnología (CINN) (ANPCyT - Argentina).

References

(1) Martin, C. R.; Siwy, Z. *Science* **2007**, *317*, 331–332.
(2) Baker, L. A.; Bird, S. P. *Nat. Nanotechnol.* **2008**, *3*, 73–74.
(3) Sexton, L. T.; Horne, L. P.; Martin, C. R. *Mol. BioSyst.* **2007**, *3*, 667–685.
(4) Wanunu, M.; Meller, A. *Nano Lett.* **2007**, *7*, 1580–1585.
(5) Siwy, Z. *Adv. Funct. Mater.* **2006**, *16*, 735–746.
(6) Gyurcsányi, R. E. *Trends Anal. Chem.* **2008**, *27*, 627–639.
(7) Siwy, Z.; Gu, Y.; Spohr, H. A.; Baur, D.; Wolf-Reber, A.; Spohr, R.; Apel, P.; Korchev, Y. E. *Europhys. Lett.* **2002**, *60*, 349–355.
(8) Lev, A. A.; Korchev, Y. E.; Rostovtseva, T. K.; Bashford, C. L.; Edmonds, D. T.; Pasternak, C. A. *Proc. R. Soc. B* **1993**, *252*, 187–192.

(9) (a) Li, J.; Stein, D.; McMullan, C.; Branton, D.; Aziz, M. J.; Golovchenko, J. A. *Nature* **2001**, *412*, 166–169. (b) Ho, C.; Heng, J. B.; Chatterjee, A.; Timp, R. J.; Aluru, N. R.; Timp, G. *Proc. Natl. Acad. Sci. U.S.A.* **2005**, *102*, 10445–10450.
(10) Spohr, R. *Radiat. Meas.* **2005**, *40*, 191–202.
(11) Stein, D.; Kruithof, M.; Dekker, C. *Phys. Rev. Lett.* **2004**, *93*, 035901.
(12) Siwy, Z.; Heins, E.; Harrell, C. C.; Kohli, P.; Martin, C. R. *J. Am. Chem. Soc.* **2004**, *126*, 10850–10851.
(13) (a) Cervera, J.; Schiedt, B.; Neumann, R.; Mafé, S.; Ramírez, P. *J. Chem. Phys.* **2006**, *124*, 104706. (b) Liu, Q.; Wang, Y.; Guo, W.; Ji, H.; Xue, J.; Ouyang, Q. *Phys. Rev. E* **2007**, *75*, 051201. (c) Kosińska, I. D.; Goychuk, I.; Kostur, M.; Schmid, G.; Hänggi, P. *Phys. Rev. E* **2008**, *77*, 031131. (d) Ali, M.; Schiedt, B.; Healy, K.; Neumann, R.; Ensinger, W *Nanotechnology* **2008**, *19*, 085713. (e) Vlassiouk, I.; Siwy, Z. *Nano Lett.* **2007**, *7*, 552–556. (f) Höltzel, A.; Tallarek, U. *J. Sep. Sci.* **2007**, *30*, 1398–1419.
(14) (a) Karnik, R.; Fan, R.; Yue, M.; Li, D.; Yang, P.; Majumdar, A *Nano Lett.* **2005**, *5*, 943–948. (b) Daiguji, H.; Yang, P.; Majumdar, A. *Nano Lett.* **2004**, *4*, 137–142.
(15) (a) Siwy, Z.; Apel, P.; Baur, D.; Dobrev, D. D.; Korchev, Y. E.; Neumann, R.; Spohr, R.; Trautmann, C.; Voss, K.-O *Surf. Sci.* **2003**, *532*−*535*, 1061–1066. (b) Dekker, C. *Nat. Nanotechnol.* **2007**, *2*, 209–215. (c) Gin, M. S.; Schmidt, E. G.; Taludkar, P. In *Nanobiotechnology II: More Concepts and Applications*; MirkinC., NiemeyerC., Eds.; Wiley-VCH: Weinheim, 2007; Chapter 1, pp 3−16.
(16) (a) Wei, C.; Bard, A. J.; Feldberg, S. W. *Anal. Chem.* **1997**, *69*, 4627–4633. (b) Siwy, Z.; Fulinski, A *Phys. Rev. Lett.* **2002**, *89*, 198103–1/4.
(17) Kalman, E. B.; Vlassiouk, I.; Siwy, Z. *Adv. Mater.* **2008**, *20*, 293–297.
(18) (a) Beckstein, O.; Sansom, M. S. P. *Phys. Biol.* **2004**, *1*, 42–52. (b) Beckstein, O.; Sansom, M. S P. *Phys. Biol.* **2006**, *3*, 147–159. (c) Bashford, C. L. *Eur. Biophys. J.* **2004**, *33*, 280–282.
(19) Bayley, H.; Braha, O.; Cheley, S.; Gu, L.-Q. In *Nanobiotechnology: Concepts, Applications and Perspectives*; Niemeyer, C., Mirkin, C.; Eds.; Wiley-VCH: Weinheim, 2004; Chapter 7, pp 93−112.
(20) Goodsell, D. S. In *Bionanotechnology: Lessons from Nature*; Wiley-LISS: Hoboken, NJ, 2004; Chapter 5, p 205.
(21) (a) Pinto, L. H.; Holsinger, L. J.; Lamb, R. A. *Cell* **1992**, *69*, 517–528. (b) Kass, I.; Arkin, I. T. *Structure* **2005**, *13*, 1789–1798.
(22) (a) Okada, A.; Miura, T.; Takeuchi, H. *Biochemistry* **2001**, *40*, 6053–6060. (b) Takeuchi, H; Okada, A.; Miura, T *FEBS Lett.* **2003**, *552*, 35–38.
(23) (a) Yameen, B.; Ali, M.; Neumann, R.; Ensinger, W.; Knoll, W.; Azzaroni, O. *J. Am. Chem. Soc.* **2009**, *131*, 2070–2071. (b) Calvo, A.; Yameen, B; Williams, F. J.; Azzaroni, O.; Soler-Illia, G. J. A. A. *Chem. Comm.* **2009**, 2553–2555.
(24) *Polymer Brushes: Synthesis, Characterization and Applications*; Advincula, R. C., Brittain, W. J., Caster, K. C., Rühe, J., Eds.; Wiley-VCH: Weinheim, 2004.
(25) (a) *Responsive Polymer Materials: Design and Applications*; Minko, S., Ed.; Blackwell Publishing: Ames, IA, 2006.
(26) (a) Azzaroni, O.; Brown, A. A.; Huck, W. T. S. *Angew. Chem., Int. Ed.* **2006**, *45*, 1770–1774. (b) Azzaroni, O.; Brown, A. A.; Huck, W. T. S. *Adv. Mater.* **2007**, *19*, 151–154. (c) Brown, A. A.; Azzaroni, O.; Huck, W.T. S. *Langmuir* **2009**, *25*, 1744–1749. (d) Yameen, B.; Ali, M.; Neumann, R.; Ensinger, W.; Knoll, W.; Azzaroni, O. *Small* **2009**, *5*, 1287–1291.
(27) (a) Chtanko, N.; Toimil Molares, M. E.; Cornelius, T.; Dobrev, D.; Neumann, R. *J. Phys. Chem. B* **2004**, *108*, 9950–9954. (b) Apel, P.; Blonskaya, I. V.; Yu, A.; Dmitriev, S. N.; Orelovitch, O. L.; Root, D.; Samoilova, L. I.; Vutsadakis, V. A. *Nucl. Instrum. Methods Phys. Res., Sect. B* **2001**, *179*, 55–62.
(28) Prucker, O.; Rühe, J. *Langmuir* **1998**, *14*, 6893–6898.
(29) Huang, W.; Skanth, G.; Baker, G. L.; Bruening, M. L. *Langmuir* **2001**, *17*, 1731–1736.
(30) (a) Ren, Y.; Jiang, X.; Yin, J. *Eur. Polym. J.* **2008**, *44*, 4108–4114. (b) Xu, Y.; Shi, L.; Ma, R.; Zhang, W.; An, Y.; Zhu, X. X. *Polymer* **2007**, *48*, 1711–1717.
(31) Su, X.; Li, Q.; Shrestha, K.; Cormet-Boyaka, E.; Chen, L.; Smith, P. R.; Sorscher, E. J.; Benos, D. J.; Matalon, S.; Ji, H. L. *J. Biol. Chem.* **2006**, *281*, 36960–36968.
(32) Tam, T. K.; Ornatska, M.; Pita, M.; Minko, S.; Katz, E. *J. Phys. Chem. C* **2008**, *112*, 8438–8445.
(33) Lindqvist, J.; Nyström, D.; Östmark, E.; Antoni, P.; Carlmark, A.; Johansson, M.; Hult, A.; Malmström, E. *Biomacromolecules* **2008**, *9*, 2139–2145.
(34) (a) Vlassiouk, I.; Park, C.-D.; Vail, S. A.; Gust, D.; Smirnov, S. *Nano Lett.* **2006**, *6*, 1013–1017. (b) Kocer, A.; Walko, M.; Meijberg, W.; Feringa, B. L. *Science* **2005**, *309*, 755–758.
(35) Roth, R.; Gillespie, D.; Nonner, W.; Eisenberg, R. E. *Biophys. J.* **2008**, *94*, 4282–4298.
(36) Smeets, R. M. M.; Keyser, U. F.; Wu, M. Y.; Dekker, N. H.; Dekker, C. M. *Phys. Rev. Lett.* **2006**, *97*, 088101.
(37) Russo, J.; Melchionna, S.; De Luca, F.; Casieri, C. *Phys. Rev B* **2007**, *76*, 195403.

NL901403U